frontiers | Frontiers in Pediatrics

TYPE Original Research
PUBLISHED 30 March 2023
DOI 10.3389/fped.2023.1080194

Check for updates

OPEN ACCESS

EDITED BY
Yoonhae Kwak,
University of Ulsan, Republic of Korea

REVIEWED BY
Marco Sapienza,
University of Catania, Italy
Sicheng Zhang,
Anhui Provincial Children's Hospital, China
Seung-Bo Lee,
Keimyung University, Republic of Korea
Ge Zhang,
Children's Hospital of Chongqing Medical University, China

*CORRESPONDENCE
Yabo Yan
yanyabo@fmmu.edu.cn
Yi Li
yili@xidian.edu.cn

†These authors have contributed equally to this work and share first authorship

SPECIALTY SECTION
This article was submitted to Pediatric Orthopedics, a section of the journal Frontiers in Pediatrics

RECEIVED 26 October 2022
ACCEPTED 06 March 2023
PUBLISHED 30 March 2023

CITATION
Sha J, Huang L, Chen Y, Fan Z, Lin J, Yang Q, Li Y and Yan Y (2023) Clinical thought-based software for diagnosing developmental dysplasia of the hip on pediatric pelvic radiographs.
Front. Pediatr. 11:1080194.
doi: 10.3389/fped.2023.1080194

COPYRIGHT
© 2023 Sha, Huang, Chen, Fan, Lin, Yang, Li and Yan. This is an open-access article distributed under the terms of the Creative Commons Attribution License (CC BY). The use, distribution or reproduction in other forums is permitted, provided the original author(s) and the copyright owner(s) are credited and that the original publication in this journal is cited, in accordance with accepted academic practice. No use, distribution or reproduction is permitted which does not comply with these terms.

Clinical thought-based software for diagnosing developmental dysplasia of the hip on pediatric pelvic radiographs

Jia Sha[1†], Luyu Huang[1†], Yaopeng Chen[2,3], Zongzhi Fan[1], Jincong Lin[1], Qinghai Yang[2], Yi Li[2*] and Yabo Yan[1*]

[1]Department of Orthopedics, Xijing Hospital, Air Force Military Medical University, Xi'an, China, [2]School of Telecommunications Engineering, Xidian University, Xi'an, China, [3]Guangzhou Institute, Xidian University, Xi'an, China

Background: The common methods of radiographic diagnosis of developmental dysplasia of the hip (DDH) include measuring hip parameters and quantifying the degree of hip dislocation. However, clinical thought-based analysis of hip parameters may be a more effective way to achieve expert-like diagnoses of DDH. This study aims to develop a diagnostic strategy-based software for pediatric DDH and validate its clinical feasibility.
Methods: In total, 543 anteroposterior pelvic radiographs were retrospectively collected from January 2017 to December 2021. Two independent clinicians measured four diagnostic indices to compare the diagnoses made by the software and conventional manual method. The diagnostic accuracy was evaluated using the receiver operator characteristic (ROC) curves and confusion matrix, and the consistency of parametric measurements was assessed using Bland-Altman plots.
Results: In 543 cases (1,086 hips), the area under the curve, accuracy, sensitivity, and specificity of the software for diagnosing DDH were 0.988–0.994, 99.08%–99.72%, 98.07%–100.00%, and 99.59%, respectively. Compared with the expert panel, the Bland-Altman 95% limits of agreement for the acetabular index, as determined by the software, were −2.09°–2.91° (junior orthopedist) and −1.98°–2.72° (intermediate orthopedist). As for the lateral center-edge angle, the 95% limits were −3.68°–5.28° (junior orthopedist) and −2.94°–4.59° (intermediate orthopedist).
Conclusions: The software can provide expert-like analysis of pelvic radiographs and obtain the radiographic diagnosis of pediatric DDH with great consistency and efficiency. Its initial success lays the groundwork for developing a full-intelligent comprehensive diagnostic system of DDH.

KEYWORDS
developmental dysplasia of the hip, children, pelvic radiograph, diagnosis, software

1. Introduction

Developmental dysplasia of the hip (DDH) is a common skeletal deformity in children and the prominent cause of hip osteoarthritis and lower limb disability (1, 2). Early diagnosis and timely treatment of DDH are beneficial to promote normal hip development (3–5). Anteroposterior pelvic radiography is the first-line screening examination for evaluating

Abbreviations
DDH, Developmental dysplasia of the hip; AI, Acetabular index; LCEA, Lateral center-edge angle; IHDI, International Hip Dysplasia Institute; Ed, Euclidean distance; ROC, Receiver operator characteristic; ICC, Intra-class correlation coefficient.

DDH in children over 4–6 months (4). Dynamic splinting, represented by the Pavlik harness, is the preferred therapeutic option for children under six months with reducible DDH; static bracing (e.g., the rhino brace) is for children over 6–9 months with DDH needing continued abduction positioning (6).

Improper interpretation of pelvic radiographs may misdiagnose pediatric DDH, impair the hip's development, and cause long-term joint dysfunction (7, 8). As machine learning developed, several scholars began trying to apply artificial intelligence algorithms to assist in diagnosing DDH (9–13). This technique is practical but still in its infancy (3). Its limitations include inaccuracy in locating key landmarks, absence of diagnostic criteria, and failure to achieve an integrated diagnosis by considering the correlation between parameter values and their clinical significance (9, 14–16).

However, clinical experts' diagnosis of DDH requires the patient-centered analysis and judgment of hip parameters by combining medical knowledge and personal information (i.e., clinical thought) (17–19). Additionally, the immaturity of pediatric hips leads to significant variation in the morphology of anatomical landmarks among children of different ages, especially in DDH (8, 20). Therefore, it is challenging to rely solely on machine learning to locate anatomical landmarks in children. The clinical diagnosis of DDH still relies primarily on manual labeling, measurement, and analysis methods.

This study developed and validated a diagnostic strategy-based software for DDH against the above issues, prioritizing accuracy while pursuing efficiency. To our knowledge, the proposed software was the first attempt to integrate the diagnostic strategy of pediatric DDH into the evaluation of anteroposterior pelvic radiographs. Firstly, the end-user manually annotated anatomical key points on pelvic radiographs. Then some points deviating from the bony rim were rectified based on the minimum Euclidean distance. Next, the key points' coordinate information was used to obtain hip parameters. Finally, an integrated diagnosis of the pelvic radiograph was made *via* the built-in diagnostic strategy for DDH. The hypothesis is that the software can achieve an expert-like diagnosis of pediatric DDH quickly and accurately.

2. Methods

2.1. Patients

The retrospective studies involving human participants were reviewed and approved by the Medical Ethics Committee of the First Affiliated Hospital of the Airforce Medical University. The requirement of informed consent was waived due to the anonymous use of imaging data. The original 1,606 anonymized anteroposterior pelvic radiographs from the Radiology department of Xijing hospital between January 2017 and December 2021 were included in the study with the following inclusion criteria: (1) age of 0.4–8.0 years; (2) available pelvic radiographs covering the area from the level of the iliac crest to the mid-superior femur; (3) children with chief complaints of hip pain or suspected DDH; (4) initial visit.

During pelvic radiography, the children were instructed in a standard anteroposterior supine position with both lower extremities internally rotated by 15° (21). The exclusion criteria for ineligible cases were radiographs with (1) extreme tilt or rotation according to Tönnis criteria (the rotation quotient or symphyseal-ischial angle exceeded the reference range) (22), (2) previous history of hip surgery, (3) traumatic or infectious hip deformities, and (4) other congenital hip deformities such as Legg-Calvé-Perthes disease. There were 543 radiographs finally incorporated into the study (**Table 1**).

2.2. Built-in diagnostic strategy for DDH

In this study, the acetabular index of Hilgenreiner (AI) was used to assess acetabular development in children (23). Its normal range was influenced by the child's nationality, gender, age, and bilateral differences (17, 18). Meanwhile, Wiberg's lateral center-edge angle (LCEA) was chosen to assess the acetabular coverage (24). Pediatric DDH was diagnosed when AI exceeded double standard deviations from the mean ($\bar{x} + 2s$). Different criterias depending on the nationality (Zhao's and Tönnis' criteria for Chinese and non-Chinese, respectively) were adopted (17, 18). Furthermore, the International Hip Dysplasia Institute (IHDI) radiographic classification was used to quantify the severity of DDH (25–27). The relative position of the midpoint of the proximal femoral metaphysis (H-point) further classified pediatric DDH into IHDI grade 1 to 4 hips. Non-DDH were then divided into normal and other dislocated hips (e.g., neurogenic dislocation of the hip) according to the presence or absence of hip dislocation. The detailed diagnostic strategy for pediatric DDH is shown in **Figure 1** and **Table 2**.

2.3. Application implementation

The proposed computer-aided software used a three-step approach to diagnose pediatric DDH from pelvic radiographs

TABLE 1 Patient demographics and radiographic diagnosis.

Parameter	Value
Cases (*n*)	543
Gender, F: M (*n*)	408:135
Mean age (years)	2.0 (95%CI 0.6–4.3)
Age, *n*	
0–2 years	330
≥2 years	213
Diagnosis (hips)	
Non-DDH	723
Normal	715
Other	8
DDH (IHDI classification)	363
Grade 1	128
Grade 2	62
Grade 3	63
Grade 4	110

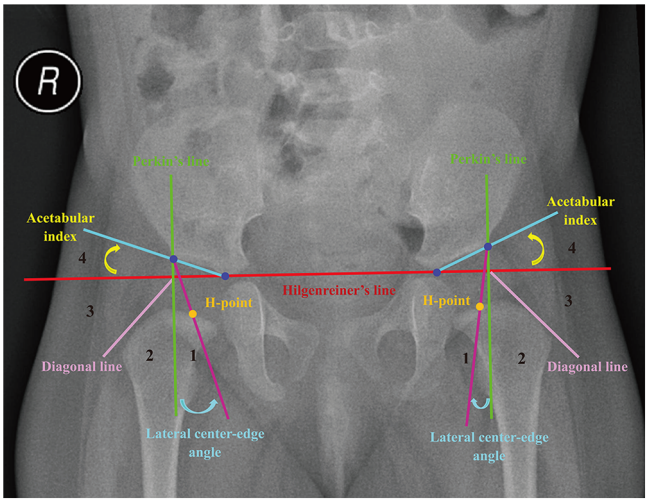

FIGURE 1
Diagnostic references of developmental dysplasia of the hip (relies on the midpoint of the proximal femoral metaphysis, H-point). Hilgenreiner's line is a basal line connecting the top of bilateral triradiate cartilages. Perkin's line is perpendicular to Hilgenreiner's line, passing through the lateral acetabular edge. The diagonal line is drawn 45 degrees from the junction of Perkin's line and Hilgenreiner's line. The acetabular index is the angle between Hilgenreiner's line and the line from the top of the triradiate cartilage to the lateral acetabular edge. Lateral center-edge angle is the angle between a vertical line through the center of the femoral head and a line connecting that center and the lateral acetabular edge.

TABLE 2 The radiographic diagnosis for pediatric developmental dysplasia of the hip.

Diagnosis	Description
DDH	Abnormal acetabular index
IHDI 1	The midpoint of the proximal femoral metaphysis (H-point) is at or medial to Perkin's line.
IHDI 2	H-point is lateral to Perkin's line and at or medial to the diagonal line.
IHDI 3	H-point is lateral to the diagonal line and at or inferior to Hilgenreiner's line.
IHDI 4	H-point is superior to Hilgenreiner's line.
Non-DDH	Normal acetabular index
Normal	Non-dislocated hip
Other	Other hip dislocation (e.g., neurogenic dislocation of the hip)

The diagonal line is drawn 45 degrees from the junction of Perkin's line and Hilgenreiner's line.

(Figure 2). For the first step, the end-user manually annotated anatomical key points on pelvic radiographs to obtain their initial coordinates (x, y). The key points included the lateral acetabular edge, the top of the triradiate cartilage, and the inner and outer points of the proximal femoral metaphysis. For some points deviating from the bony rim, the computer intercepted an area of 30×30 pixels around them and turned the area into a grayscale image. After the processes of Gaussian filtering, adaptive threshold, and edge detection, the bony rim was identified. Then the Euclidean distance (Equation 1) from the initial annotated point (x, y) to the rim was calculated. After that, the pixel point on the rim (a, b) that minimizes the Ed was selected as the rectified annotated point.

$$\mathrm{Ed} = \sqrt{(x-a)^2 + (y-b)^2} \quad (1)$$

In the second step, diagnostic references (e.g., the H-point, Hilgenreiner's line, and Perkin's line) were drawn based on the annotated points' coordinates. Then the acetabulum-head relationship and hip parameters were measured automatically. The third step was to input a child's general information (i.e., nationality, gender, and age) by the end-user to select the appropriate diagnostic criteria for DDH. Subsequently, an expert-like radiographic diagnosis on the pelvic radiograph was performed using the built-in diagnostic strategy of pediatric DDH.

2.4. Performance testing

The AI, LCEA, overall diagnosis (non-DDH and DDH), and specific classification (normal, other dislocated, and IHDI grade 1–4 hips) were calculated to evaluate the diagnostic performance between the software and conventional manual method. Two senior pediatric orthopedists and two senior pediatric radiologists were invited to form an expert panel. Using their undisputed diagnostic results as the standard, the other two independent orthopedists measured these indices to compare the performance difference between the two methods. The two orthopedists include an intermediate orthopedist (attending surgeon) and a junior orthopedist (resident surgeon). To evaluate intra-reliability, they measured each diagnostic index twice at 4-week intervals. Besides, the difference in time consumption between the two methods was compared.

The image analysis software Digimizer 5.7.2 (MedCalc Software, Ostend, Belgium) was used to simulate the conventional manual assessment of pelvic radiographs. The main steps were as follows: (1) marking the top of bilateral triradiate

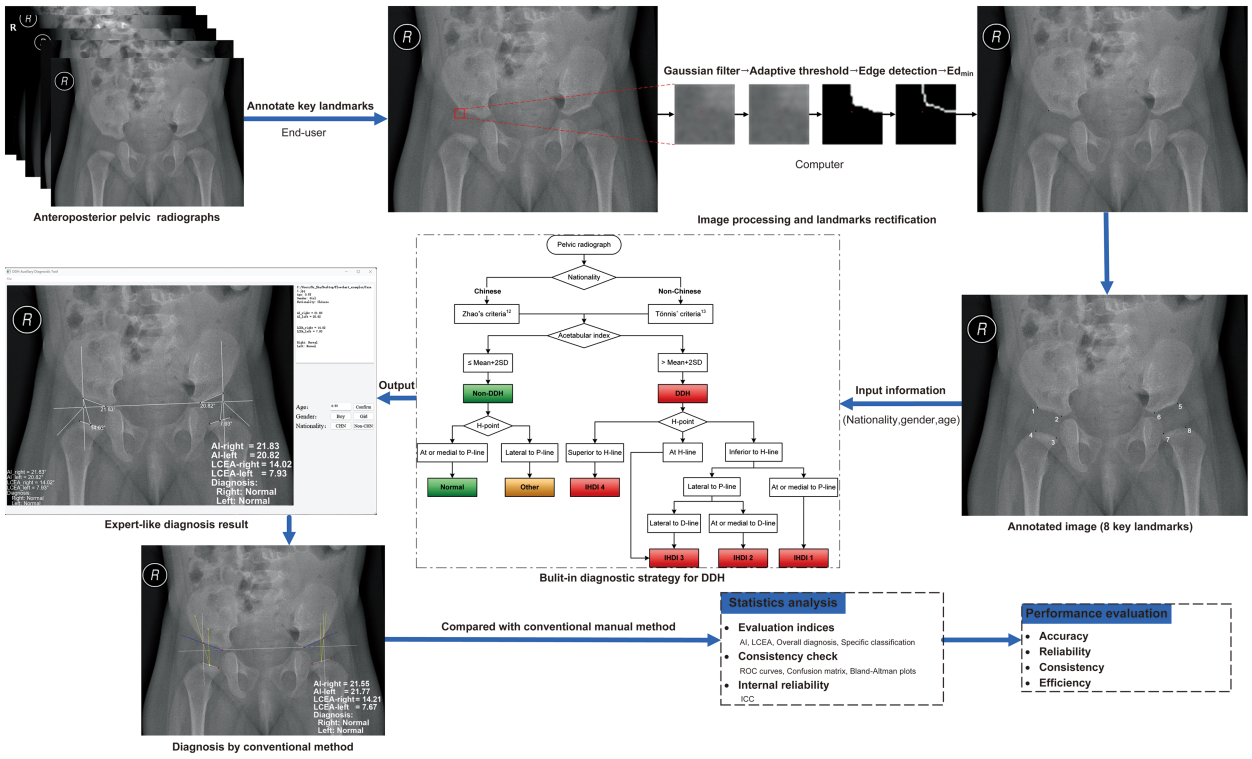

FIGURE 2
Detailed workflow of the proposed software for developmental dysplasia of the hip.

cartilage, the lateral acetabular edge, and H-point, (2) drawing Hilgenreiner's line, Perkin's line, and the diagonal line, (3) calculating the AI, LCEA, and IHDI classifications, (4) making final judgments.

2.5. Statistical analysis

The receiver operating characteristic (ROC) curves or confusion matrices were used to compare the categorical variables (i.e., the overall diagnosis and specific classification) obtained by the expert panel and two orthopedists. The areas under the ROC curves (AUCs) of the two diagnostic methods were compared using DeLong's test (28). The Bland-Altman plots and independent t-tests were then conducted to assess the agreement of continuous variables (i.e., AI and LCEA) measured by the expert panel and two orthopedists.

The test-retest reliabilities of continuous and categorical variables were quantified by the intra-class correlation coefficient (ICC) (29) and Cohen's linear weighted kappa (30), respectively. The ICCs greater than 0.80 were considered perfect agreement (31). A kappa statistic greater than 0.80 was considered satisfactory. Statistical significance was set at $p < 0.05$. All data were statistically analyzed using SPSS 28.0 (IBM, Armonk, United States) and GraphPad Prism 9.3.1 (GraphPad, San Diego, United States).

3. Results

3.1. Diagnostic effect evaluation

Four diagnostic indicators (AI, LCEA, overall diagnosis, and specific classification) of 543 pelvic radiographs (1,086 hips) were compared by two independent orthopedists using the software and conventional method. Selected examples of the software for diagnosing DDH are shown in **Figure 3**. In the conventional group, the AUC, accuracy, sensitivity, and specificity of the junior orthopedist were 0.894, 90.79% (986/1,086), 85.12% (309/363), and 93.64% (677/723), respectively. And these for the intermediate orthopedist were 0.957, 95.67% (1,039/1,086), 95.87% (348/363), and 95.57% (691/723), respectively. In the software group, the AUC was 0.988–0.994, accuracy was 99.08% (1,076/1,086)–99.72% (1,083/1,086), sensitivity was 98.07% (356/363)–100.00% (363/363), and specificity was 99.59% (720/723) (**Figure 4**). DeLong's test showed that the software was more effective than the conventional method in diagnosing DDH ($p < 0.001$). Moreover, the confusion matrix shows the diagnostic performance of the specific classification on the software was similar to the standard (**Figure 5**).

The distribution of hip parameters measured by two orthopedists compared to the standard is shown in **Figure 6**. In the conventional group, the 95% limits of agreement (Bland-Altman analyses), for AI measurements, in the junior and intermediate orthopedists were −3.26°–6.15° (bias 1.45°, $p = 0.522$) and −3.29°–3.74° (bias 0.23°, $p = 0.509$), respectively. For

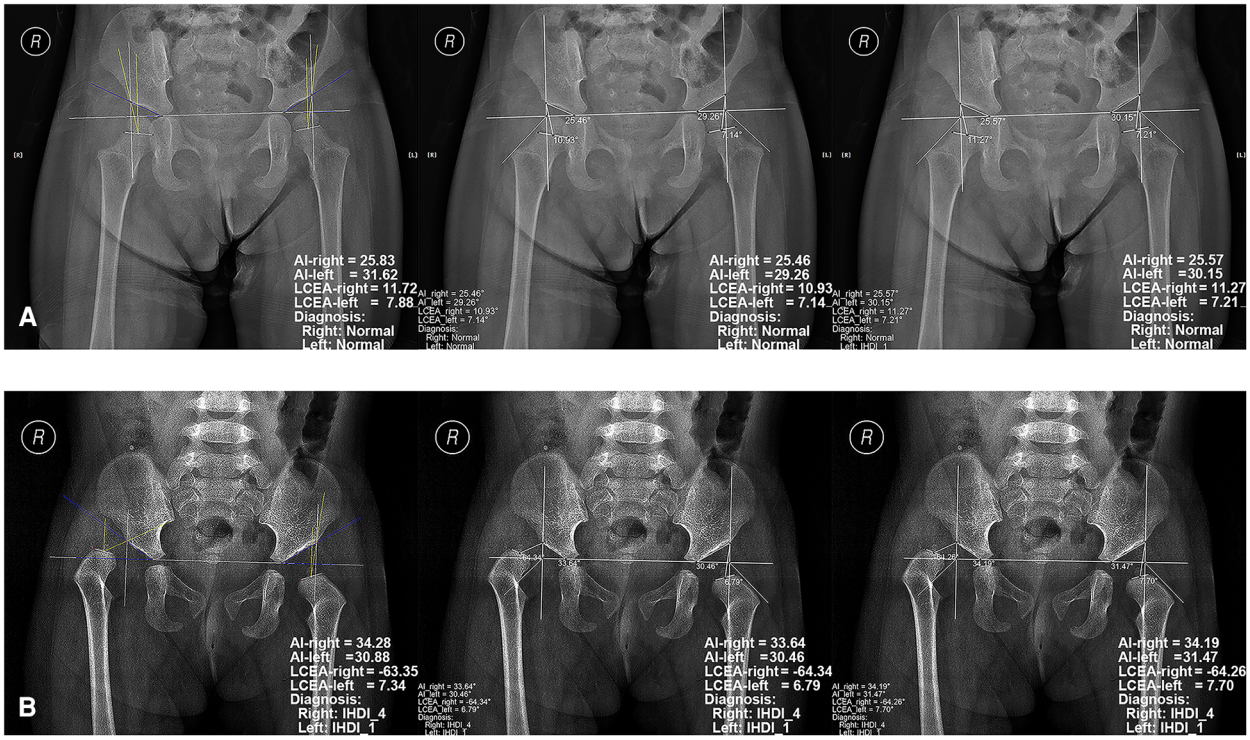

FIGURE 3
Examples of radiographic diagnosis of developmental dysplasia of the hip on pelvic radiographs by the software. The left images represent the evaluation results of the standard, while the middle and right images represent those of the software by Junior orthopedist and Intermediate orthopedist, respectively. (**A**) the pelvic radiograph of a 2.3-year-old girl; (**B**) the pelvic radiograph of a 1.4-year-old girl.

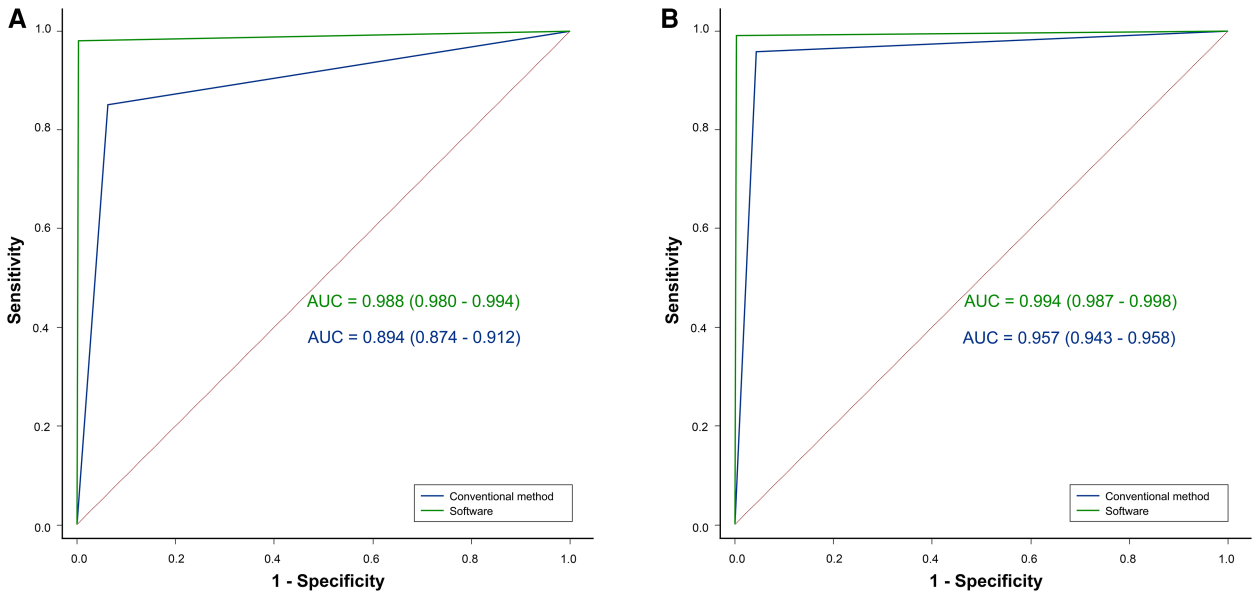

FIGURE 4
ROC analysis showing that the diagnostic performance of the software (green line) was better than that of the conventional method (blue line) in both the (**A**) junior and (**B**) intermediate orthopedists.

LCEA measurements, the 95% limits of agreement were −7.12°–11.60° (bias 2.24°, $p = 0.079$) and −7.65°–6.64° (bias −0.50°, $p = 0.690$), separately. In the software group, as for AI measurements, the 95% limits of agreement were −2.09°–2.91° (bias 0.41°, $p = 0.216$) and −1.98°–2.72° (bias 0.37°, $p = 0.264$), respectively. With regards to LCEA measurements, the 95% limits were −3.68°–5.28° (bias −0.80°, $p = 0.522$) and −2.94°–4.59° (bias −0.83°, $p = 0.509$), separately.

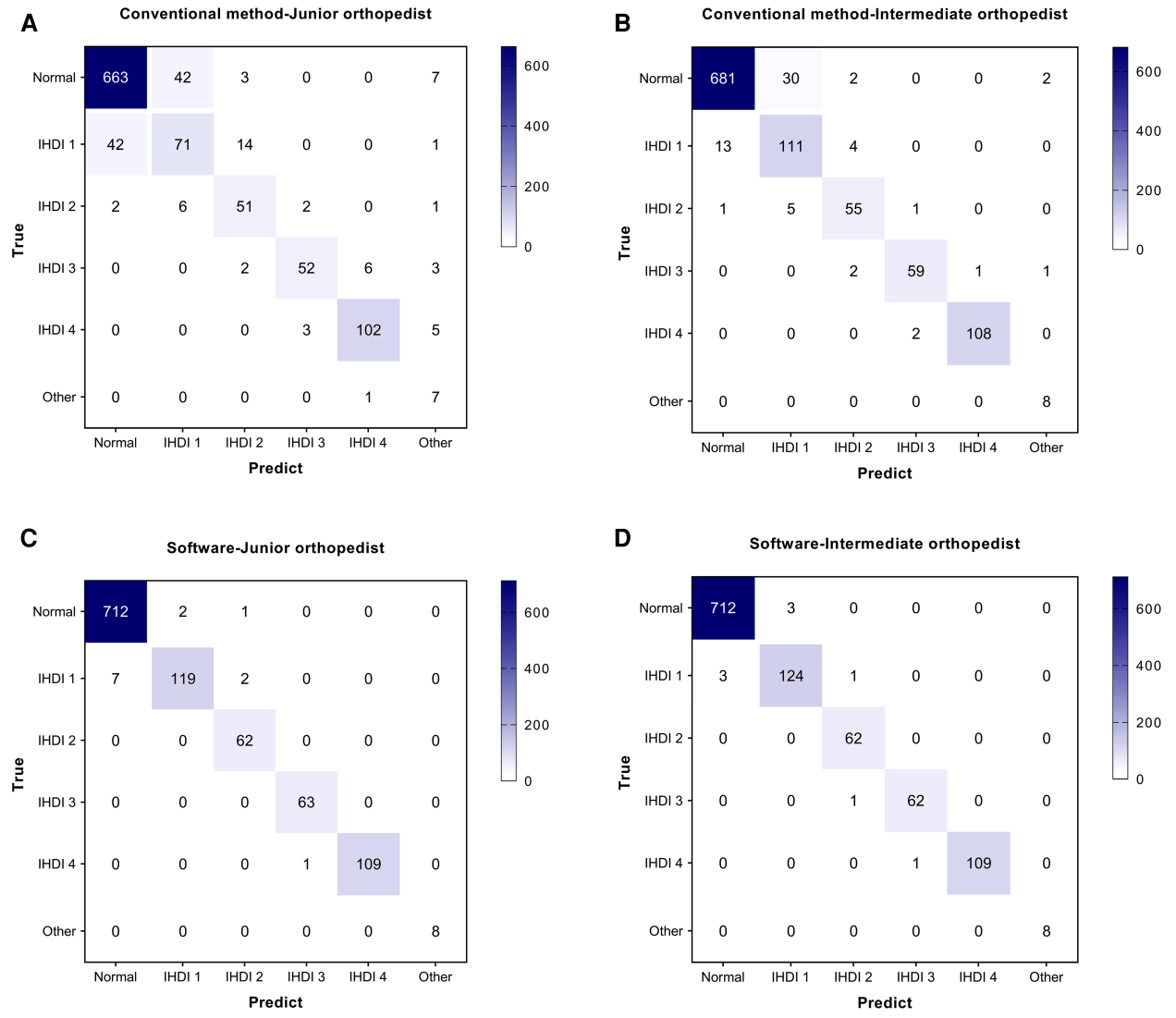

FIGURE 5
Confusion matrix of the specific classification in two orthopedists. (A) The confusion matrix of the conventional method by Junior orthopedist. (B) The confusion matrix of the conventional method by Intermediate orthopedist. (C) The confusion matrix of the software by Junior orthopedist. (D) The confusion matrix of the software by Intermediate orthopedist.

3.2. Test-retest agreement

In the conventional group, ICC values were 0.929–0.952 (AI) and 0.986- 0.993 (LCEA), and kappa values were 0.817–0.844 (overall diagnosis) and 0.904–0.919 (specific classification), while in the software group, they were 0.936–0.953, 0.990–0.992, 0.926–0.939, and 0.956–0.965, respectively. **Supplementary Figure S1** shows the perfect test-retest agreement about four diagnostic indices in the software group.

3.3. Diagnostic time

In this study, the time consumption of assessing the pelvic radiograph included loading the image data into the proposed software or Digimizer, plotting reference lines and points, and obtaining four diagnostic indices of pediatric DDH. For each case of 543 radiographs, the mean time consumption of the software (junior orthopedist, 10.70 ± 0.68 s; intermediate orthopedist, 10.66 ± 0.70 s) was significantly less ($p < 0.001$) than that of the conventional method (junior orthopedist, 177.77 ± 8.42 s; intermediate orthopedist, 156.62 ± 7.40 s) (**Supplementary Figure S2**).

4. Discussion

Early and accurate diagnosis of pediatric DDH is closely related to favorable treatment outcomes (32). Once diagnosed with DDH, treatment should be prompt to avoid serious consequences (33). Clinicians usually resort to medical image analysis because of the atypical symptoms of DDH in young children. Numerous

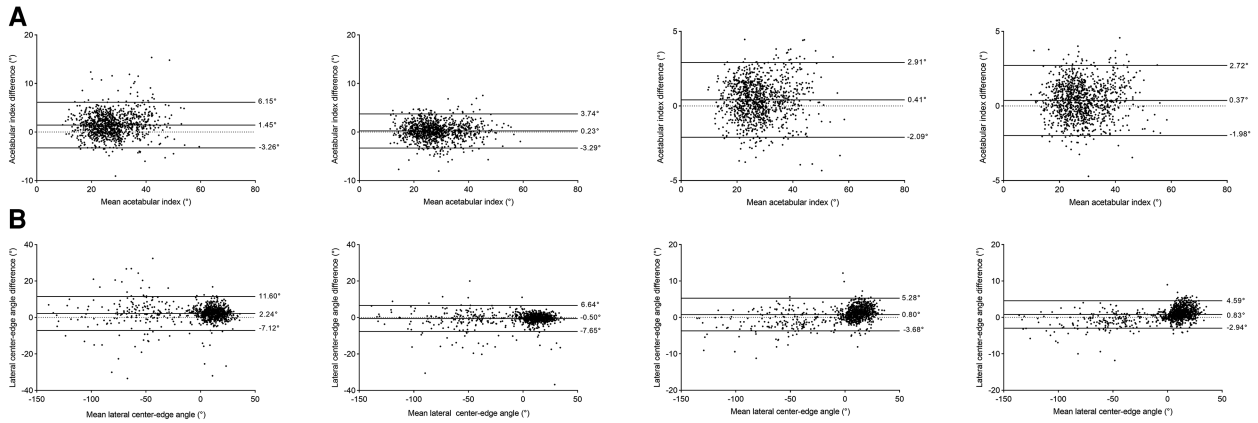

FIGURE 6
Diagnostic performance of two methods for parametric measurements using Bland-Altman plots. Two images on the left represent the diagnoses of the conventional group (for junior and intermediate orthopedists, respectively), whereas two images on the right represent the diagnoses of the software group (for junior and intermediate orthopedists, respectively). (A) acetabular index. (B) lateral center-edge angle.

auxiliary approaches have been developed recently to help clinicians diagnose DDH (9, 11, 34). These approaches focused on measuring hip parameters and determining the degree of hip dislocation. However, the clinical expert's diagnosis of pediatric DDH on pelvic radiographs requires a comprehensive analysis of whether hip parameters are abnormal by considering patients' personal information.

Compared to the experts, existing diagnostic tools lack a diagnostic strategy for DDH (9, 11, 14, 15, 25). Meanwhile, these tools may have limitations in the radiographic diagnosis of DDH. They seem to have overlooked other dislocated hips, such as hip arthochalasis and neurogenic dislocation of the hip (NDH) (35). Therefore, they were difficult to be promoted as practical diagnostic methods. In our software, the diagnostic results of pelvic radiographs were divided into normal, dysplastic, and other dislocated hips.

Previous research has revealed that the errors of inter- and intra-observer measurements in AI varied from ±3.5° to ±6.1° (36–38). These errors may be increased due to the influence of pelvic malpositioning in three-dimensional planes on the projected image (39, 40). Even artificial intelligence-assisted methods could have about ±5° errors in AI values (9, 11, 15). By contrast, the 95% limits of agreement of AI for the proposed software were −2.09°–2.91° (bias 0.409). Our results demonstrate that the software accurately diagnosed DDH in 1,076–1,083 out of 1,086 hips (99.08%–99.72%). Overall, three cases (3 hips) were diagnosed as DDH by the software but not by the expert panel. In two of these hips, detecting the lateral acetabular edge was challenging because of potential pelvic tilt. Another hip, with a high-normal AI, was misdiagnosed with DDH due to the software's measurement error. Besides, in the software group, two (3 hips) and six cases (7 hips) were misdiagnosed with normal hips by the intermediate and the junior orthopedist, respectively. Two cases (3 hips) were borderline dysplastic hips with mild abnormal AI (**Supplementary Figure S3**). The other four false-negative cases (4 hips) were difficult to locate the top of the triradiate cartilage due to pelvic rotation and tilt. Therefore, the hip MRI would be recommended in some borderline cases to investigate the acetabular development.

Despite numerous hip parameters, there is no universal diagnostic strategy for pediatric DDH (41). Previous studies revealed that DDH began with a shallow acetabulum and anteverted femur (8, 42). Sherman et al. found AI was an objective and preferred index for diagnosing hip dysplasia in children under eight (43). Davila-Parrilla et al. observed AI was a reliable parameter for assessing acetabular morphology (41). Novais et al. highlighted AI as a golden indicator to determine the severity and prognosis of DDH (44). However, AI is an age-dependent index as the child's pelvis gradually develops (17). Tönnis and Zhao et al. found that AI values were influenced by the patient's nationality, age, gender, and bilateral difference (17, 18). Thus, the present study used AI to assess acetabular development and considered those factors while diagnosing DDH.

Additionally, a specific diagnosis of DDH requires further evaluation of the acetabular-head relationship. The femoral ossific nucleus exhibited significant differences among children under three due to incomplete ossification (20). This phenomenon was more evident in DDH because of the delayed appearance and eccentricity of the ossific nucleus (42). In contrast to the Tönnis method, the IHDI classification relies on the midpoint of the proximal femoral metaphysis, which can be applied to children of all ages (27). Therefore, the IHDI classification was used to evaluate the severity of DDH.

4.1. Limitations

There are some limitations of the current study. First of all, there were a limited number of radiographs used in this study. Although only 543 radiographs were available, the proportion of cases with different diagnostic types and various age groups was reasonable. Secondly, the diagnostic strategy adopted in this

study was affected by the triradiate cartilage. Therefore, the software may not be generalized to children with a history of hip surgery or premature closure of triradiate cartilage. In addition, the proposed software could not screen standard pelvic radiographs (i.e., detecting potential pelvic malpositions). In the next version, the software will be added to the quality assessment of radiographs based on Tönnis' pelvic rotation and tilt criteria (45). Lastly, the software is a semi-automatic diagnostic tool for pediatric DDH. Although this software can help clinicians significantly improve the diagnostic accuracy of DDH, it is still user-dependent. In the subsequent research, the existing deep-learning algorithms will be optimized and integrated with this tool to develop a full-intelligent comprehensive tool for diagnosing pediatric DDH.

4.2. Conclusion

In summary, this study suggests the software can provide expert-like analysis of pelvic radiographs and obtain the radiographic diagnosis of pediatric DDH with great consistency and efficiency. Its initial success lays the groundwork for developing a full-intelligent comprehensive diagnostic system of DDH.

Data availability statement

The original contributions presented in the study are included in the article/**Supplementary Material**, further inquiries can be directed to the corresponding author/s.

Ethics statement

The retrospective studies involving human participants were reviewed and approved by the Medical Ethics Committee of the First Affiliated Hospital of the Airforce Medical University.

Author contributions

JS, LH, YC, YL, and YY: study concept and design. JS, YC, YL, and YY: software development. JS, LH, and YY: critical revisions of the manuscript for important intellectual content. JS: drafting of the manuscript. All authors reviewed the results and approved the final version of the manuscript.

Funding

This study was supported by a Grant-in-Aid for Scientific Research from the Natural Science Foundation of Shaanxi Province, China (2017JC2-04).

Conflict of interest

The authors declare that the research was conducted in the absence of any commercial or financial relationships that could be construed as a potential conflict of interest.

Publisher's note

All claims expressed in this article are solely those of the authors and do not necessarily represent those of their affiliated organizations, or those of the publisher, the editors and the reviewers. Any product that may be evaluated in this article, or claim that may be made by its manufacturer, is not guaranteed or endorsed by the publisher.

Supplementary material

The Supplementary Material for this article can be found online at: https://www.frontiersin.org/articles/10.3389/fped.2023.1080194/full#supplementary-material.

References

1. Schmitz MR, Murtha AS, Clohisy JC. Developmental dysplasia of the hip in adolescents and young adults. *J Am Acad Orthop Surg.* (2020) 28:91–101. doi: 10.5435/jaaos-d-18-00533

2. Agricola R, Heijboer MP, Roze RH, Reijman M, Bierma-Zeinstra SM, Verhaar JA, et al. Pincer deformity does not lead to osteoarthritis of the hip whereas acetabular dysplasia does: acetabular coverage and development of osteoarthritis in a nationwide prospective cohort study (CHECK). *Osteoarthritis Cartilage.* (2013) 21:1514–21. doi: 10.1016/j.joca.2013.07.004

3. Canavese F, Castañeda P, Hui J, Li L, Li Y, Roposch A. Developmental dysplasia of the hip: promoting global exchanges to enable understanding the disease and improve patient care. *Orthop Traumatol Surg Res.* (2020) 106:1243–4. doi: 10.1016/j.otsr.2020.09.004

4. Dezateux C, Rosendahl K. Developmental dysplasia of the hip. *Lancet.* (2007) 369:1541–52. doi: 10.1016/s0140-6736(07)60710-7

5. Harris NH, Lloyd-Roberts GC, Gallien R. Acetabular development in congenital dislocation of the hip. With special reference to the indications for acetabuloplasty and pelvic or femoral realignment osteotomy. *J Bone Joint Surg Br.* (1975) 57:46–52. doi: 10.1302/0301-620X.57B1.46

6. Pavone V, de Cristo C, Vescio A, Lucenti L, Sapienza M, Sessa G, et al. Dynamic and static splinting for treatment of developmental dysplasia of the hip: a systematic review. *Children (Basel).* (2021) 8:104. doi: 10.3390/children8020104

7. O'Brien T, Barry C. The importance of standardised radiographs when assessing hip dysplasia. *Ir Med J.* (1990) 83:159–61. PMID: 2081675.

8. Barrera CA, Cohen SA, Sankar WN, Ho-Fung VM, Sze RW, Nguyen JC. Imaging of developmental dysplasia of the hip: ultrasound, radiography and magnetic resonance imaging. *Pediatr Radiol.* (2019) 49:1652–68. doi: 10.1007/s00247-019-04504-3

9. Zhang SC, Sun J, Liu CB, Fang JH, Xie HT, Ning B. Clinical application of artificial intelligence-assisted diagnosis using anteroposterior pelvic radiographs in children with developmental dysplasia of the hip. *Bone Joint J.* (2020) 102-b:1574–81. doi: 10.1302/0301-620x.102b11.Bjj-2020-0712.R2

10. Yang W, Ye Q, Ming S, Hu X, Jiang Z, Shen Q, et al. Feasibility of automatic measurements of hip joints based on pelvic radiography and a deep learning algorithm. *Eur J Radiol.* (2020) 132:109303. doi: 10.1016/j.ejrad.2020.109303

11. Xu W, Shu L, Gong P, Huang C, Xu J, Zhao J, et al. A deep-learning aided diagnostic system in assessing developmental dysplasia of the hip on pediatric pelvic radiographs. *Front Pediatr*. (2021) 9:785480. doi: 10.3389/fped.2021.785480

12. Park HS, Jeon K, Cho YJ, Kim SW, Lee SB, Choi G, et al. Diagnostic performance of a new convolutional neural network algorithm for detecting developmental dysplasia of the hip on anteroposterior radiographs. *Korean J Radiol*. (2021) 22:612–23. doi: 10.3348/kjr.2020.0051

13. Li Q, Zhong L, Huang H, Liu H, Qin Y, Wang Y, et al. Auxiliary diagnosis of developmental dysplasia of the hip by automated detection of Sharp's angle on standardized anteroposterior pelvic radiographs. *Medicine (Baltimore)*. (2019) 98: e18500. doi: 10.1097/md.0000000000018500

14. Al-Bashir AK, Al-Abed M, Abu Sharkh FM, Kordeya MN, Rousan FM. Algorithm for automatic angles measurement and screening for developmental dysplasia of the hip (DDH). *Annu Int Conf IEEE Eng Med Biol Soc*. (2015) 2015:6386–9. doi: 10.1109/embc.2015.7319854

15. Liu C, Xie H, Zhang S, Mao Z, Sun J, Zhang Y. Misshapen pelvis landmark detection with local-global feature learning for diagnosing developmental dysplasia of the hip. *IEEE Trans Med Imaging*. (2020) 39:3944–54. doi: 10.1109/tmi.2020.3008382

16. Fraiwan M, Al-Kofahi N, Ibnian A, Hanatleh O. Detection of developmental dysplasia of the hip in x-ray images using deep transfer learning. *BMC Med Inform Decis Mak*. (2022) 22:216. doi: 10.1186/s12911-022-01957-9

17. Tönnis D. Normal values of the hip joint for the evaluation of x-rays in children and adults. *Clin Orthop Relat Res*. (1976) 119:39–47. PMID: 954321.

18. Yong-yan S, Tian-jing L, Qun Z, Li-jun Z, Shijun J. [The measurements of normaI acetabular index and sharp acetabular angle in Chinese hips]. *Chin J Orthop*. (2010) 30:748–53. doi: 10.3760/cma.j.issn.0253-2352.2010.08.004

19. Faucher C. Differentiating the elements of clinical thinking. *Optom Educ*. (2011) 36:140–5.

20. Acheson RM. The Oxford method of assessing skeletal maturity. *Clin Orthop*. (1957) 10:19–39. PMID: 13561550.

21. Lim SJ, Park YS. Plain radiography of the hip: a review of radiographic techniques and image features. *Hip Pelvis*. (2015) 27:125–34. doi: 10.5371/hp.2015.27.3.125

22. Tönnis D. [Indications and time planning for operative interventions in hip dysplasia in child and adulthood]. *Z Orthop Ihre Grenzgeb*. (1985) 123:458–61. PMID: 4072348.

23. H H. [Early diagnosis and early treatment of congenital dislocation of the hip]. *Med Klin*. (1925) 21:1385–8, 1425–1389.

24. Wiberg G. Shelf operation in congenital dysplasia of the acetabulum and in subluxation and dislocation of the hip. *J Bone Joint Surg Am*. (1953) 35-a:65–80. doi: 10.2106/00004623-195335010-00007

25. Ismiarto YD, Agradi P, Helmi ZN. Comparison of interobserver reliability between junior and senior resident in assessment of developmental dysplasia of the hip severity using tonnis and international hip dysplasia institute radiological classification. *Malays Orthop J*. (2019) 13:60–5. doi: 10.5704/moj.1911.010

26. Narayanan U, Mulpuri K, Sankar WN, Clarke NM, Hosalkar H, Price CT. Reliability of a new radiographic classification for developmental dysplasia of the hip. *J Pediatr Orthop*. (2015) 35:478–84. doi: 10.1097/bpo.0000000000000318

27. Ramo BA, De La Rocha A, Sucato DJ, Jo CH. A new radiographic classification system for developmental hip dysplasia is reliable and predictive of successful closed reduction and late pelvic osteotomy. *J Pediatr Orthop*. (2018) 38:16–21. doi: 10.1097/bpo.0000000000000733

28. DeLong ER, DeLong DM, Clarke-Pearson DL. Comparing the areas under two or more correlated receiver operating characteristic curves: a nonparametric approach. *Biometrics*. (1988) 44:837–45. doi: 10.2307/2531595

29. Bartko JJ. The intraclass correlation coefficient as a measure of reliability. *Psychol Rep*. (1966) 19:3–11. doi: 10.2466/pr0.1966.19.1.3

30. Cohen J. Weighted kappa: nominal scale agreement with provision for scaled disagreement or partial credit. *Psychol Bull*. (1968) 70:213–20. doi: 10.1037/h0026256

31. Montgomery AA, Graham A, Evans PH, Fahey T. Inter-rater agreement in the scoring of abstracts submitted to a primary care research conference. *BMC Health Serv Res*. (2002) 2:8. doi: 10.1186/1472-6963-2-8

32. Kotlarsky P, Haber R, Bialik V, Eidelman M. Developmental dysplasia of the hip: what has changed in the last 20 years? *World J Orthop*. (2015) 6:886–901. doi: 10.5312/wjo.v6.i11.886

33. Yang S, Zusman N, Lieberman E, Goldstein RY. Developmental dysplasia of the hip. *Pediatrics*. (2019) 143:e20181147. doi: 10.1542/peds.2018-1147

34. Xu J, Xie H, Tan Q, Wu H, Liu C, Zhang S, et al. Multi-task hourglass network for online automatic diagnosis of developmental dysplasia of the hip. *World Wide Web*. (2023) 26:539–59. doi: 10.1007/s11280-022-01051-0

35. Milks KS, Mesi EL, Whitaker AT, Ruess L. Standardized process measures in radiographic hip surveillance for children with cerebral palsy. *Pediatr Qual Saf*. (2021) 6:e485. doi: 10.1097/pq9.0000000000000485

36. Spatz DK, Reiger M, Klaumann M, Miller F, Stanton RP, Lipton GE. Measurement of acetabular index intraobserver and interobserver variation. *J Pediatr Orthop*. (1997) 17:174–5. doi: 10.1097/00004694-199703000-00007

37. Broughton NS, Brougham DI, Cole WG, Menelaus MB. Reliability of radiological measurements in the assessment of the child's hip. *J Bone Joint Surg Br*. (1989) 71:6–8. doi: 10.1302/0301-620x.71b1.2915007

38. Boniforti FG, Fujii G, Angliss RD, Benson MK. The reliability of measurements of pelvic radiographs in infants. *J Bone Joint Surg Br*. (1997) 79:570–5. doi: 10.1302/0301-620x.79b4.7238

39. van der Bom MJ, Groote ME, Vincken KL, Beek FJ, Bartels LW. Pelvic rotation and tilt can cause misinterpretation of the acetabular index measured on radiographs. *Clin Orthop Relat Res*. (2011) 469:1743–9. doi: 10.1007/s11999-011-1781-6

40. Hamano D, Yoshida K, Higuchi C, Otsuki D, Yoshikawa H, Sugamoto K. Evaluation of errors in measurements of infantile hip radiograph using digitally reconstructed radiograph from three-dimensional MRI. *J Orthop*. (2019) 16:302–6. doi: 10.1016/j.jor.2019.05.004

41. Davila-Parrilla AD, Wylie J, O'Donnell C, Maranho DA, Carry P, Novais EN. Reliability of and correlation between measurements of acetabular morphology. *Orthopedics*. (2018) 41:e629–35. doi: 10.3928/01477447-20180711-01

42. Guille JT, Pizzutillo PD, MacEwen GD. Development dysplasia of the hip from birth to six months. *J Am Acad Orthop Surg*. (2000) 8:232–42. doi: 10.5435/00124635-200007000-00004

43. Sherman B, Lalonde FD, Schlechter JA. Measuring the acetabular Index: an accurate and reliable alternative method of measurement. *AJR Am J Roentgenol*. (2021) 217:172–6. doi: 10.2214/ajr.20.23358

44. Novais EN, Pan Z, Autruong PT, Meyers ML, Chang FM. Normal percentile reference curves and correlation of acetabular Index and acetabular depth ratio in children. *J Pediatr Orthop*. (2018) 38:163–9. doi: 10.1097/bpo.0000000000000791

45. Tönnis D. General radiography of the hip joint. In: Telger TC, ed. *Congenital Dysplasia and Dislocation of the Hip in Children and Adults*. Berlin, Heidelberg: Springer. (1987). p. 100–142. doi: 10.1007/978-3-642-71038-4